



Synthesis of GaN by N ion implantation in GaAs (001)

X. W. Lin, M. Behar, R. Maltez, W. Swider, Z. Liliental-Weber, and J. Washburn

Citation: *Applied Physics Letters* **67**, 2699 (1995); doi: 10.1063/1.114297

View online: <http://dx.doi.org/10.1063/1.114297>

View Table of Contents: <http://scitation.aip.org/content/aip/journal/apl/67/18?ver=pdfcov>

Published by the [AIP Publishing](#)

Articles you may be interested in

[Lateral damage extension during masked ion implantation into GaAs](#)

J. Appl. Phys. **80**, 4303 (1996); 10.1063/1.363378

[Characterization of stoichiometric surface and buried SiN films fabricated by ion implantation using extended x-ray absorption fine structure](#)

J. Appl. Phys. **80**, 2720 (1996); 10.1063/1.363189

[GaAs nanocrystals formed by sequential ion implantation](#)

J. Appl. Phys. **79**, 1876 (1996); 10.1063/1.361088

[MeV B compensation implants into n-type GaAs and InP](#)

J. Appl. Phys. **72**, 2179 (1992); 10.1063/1.351608

[Material-dependent amorphization and epitaxial crystallization in ion-implanted AlAs/GaAs layer structures](#)

Appl. Phys. Lett. **55**, 1211 (1989); 10.1063/1.101657

A small image of the cover of Applied Physics Reviews, showing a grid of atoms and a diagram of a device structure.

NEW Special Topic Sections

NOW ONLINE
Lithium Niobate Properties and Applications:
Reviews of Emerging Trends

AIP Applied Physics Reviews

Synthesis of GaN by N ion implantation in GaAs (001)

X. W. Lin^{a)}

Materials Science Division, Lawrence Berkeley Laboratory, University of California, Berkeley, California 94720

M. Behar and R. Maltez

Instituto de Física, UFRGS, 91501 Porto Alegre, Brazil

W. Swider, Z. Liliental-Weber, and J. Washburn

Materials Science Division, Lawrence Berkeley Laboratory, University of California, Berkeley, California 94720

(Received 24 April 1995; accepted for publication 23 August 1995)

Both the hexagonal and cubic GaN phases were synthesized in GaAs (001) by 50 keV N ion implantation at 380 °C and subsequent furnace annealing at 850–950 °C for 10 min–2 h. For a fluence of $1.5 \times 10^{17} \text{ cm}^{-2}$, transmission electron microscopy revealed that cubic GaN epitaxially crystallizes as precipitates in the GaAs matrix. A cubic-to-hexagonal GaN phase transition was observed for extended thermal anneals. By increasing the N fluence to $3 \times 10^{17} \text{ cm}^{-2}$, a continuous buried layer of randomly oriented hexagonal-GaN nanocrystals was produced. © 1995 American Institute of Physics.

Recent advances in epitaxy of high-quality GaN and the realization of GaN-based optical devices have spurred a flurry of research activity aimed at exploiting the potential of III-V nitrides (including InN, AlN, GaN, and their alloys) as light emitting devices active in the full range of the visible spectrum (blue and UV region in particular) and as electronic devices suitable for high temperature, high power, and high frequency applications.¹ To date, many techniques, including reactive sputtering, chemical vapor deposition, reactive molecular beam epitaxy, and their variations, have been used to grow GaN thin films on a variety of substrates, such as sapphire and GaAs.² GaN normally grows in its stable hexagonal phase (α -GaN) with the wurtzite structure, but a metastable cubic phase (β -GaN) of zincblende structure can also be produced under certain growth conditions.^{1–3}

In this letter, we report a novel technique of producing GaN, namely, ion-beam synthesis via N ion implantation in a GaAs substrate. This approach is based on the following considerations: first, since GaN is thermodynamically more stable than GaAs (heats of formation ≈ -109.5 and $-81.5 \text{ kJ mol}^{-1}$, respectively),⁴ introduction of N atoms in GaAs is expected to cause N–As exchange and result in GaN formation. Second, the replacement of As by N atoms is facilitated by the fact that As is more volatile than Ga and tends to escape from GaAs upon thermal annealing. Third, ion implantation is a technique that allows for substantial introduction of N atoms in GaAs, far beyond the solid solubility limit. As shown below, low-energy (50 keV), high-fluence (up to $3 \times 10^{17} \text{ cm}^{-2}$) N ion implantation in GaAs, combined with thermal treatments, can be used to produce either epitaxial cubic GaN precipitates or a continuous buried hexagonal GaN layer.

Previous x-ray photoelectron spectroscopy studies indicated that very low-energy ($\leq 3 \text{ keV}$) N^+ or N_2^+ ion-beam or plasma bombardment of a GaAs surface can lead to the for-

mation of a thin GaN surface layer.⁵ The GaN formation in those cases involves a dynamic surface reaction process, which is different from that involved in the present ion-beam synthesis.

Semi-insulating GaAs(001) wafers were implanted at 380 °C with 50 keV N to a fluence of 1.5×10^{17} or $3 \times 10^{17} \text{ cm}^{-2}$; the beam current was $1 \mu\text{A cm}^{-2}$. Rutherford backscattering spectrometry analysis indicated the occurrence of As loss upon N implantation. Furnace annealing was performed at 850 or 950 °C for 10 min–2 h under flowing N_2 gas. Samples were pieces cut from the implanted wafer; each was placed face-to-face on a large piece of virgin GaAs wafer during annealing. Structural characterization was done by cross-sectional transmission electron microscopy (TEM) on a JEOL 200CX microscope.

For a fluence of $1.5 \times 10^{17} \text{ cm}^{-2}$, N implantation results in the formation of amorphous precipitates, distributed over a surface layer $\approx 150 \text{ nm}$ thick [Fig. 1(a)]. Laterally elongated amorphous regions can be seen at the middle of the implanted layer; they are formed due to precipitate coalescence. Figure 1(b) shows a high-resolution image of a typical amorphous precipitate ($\approx 7.5 \text{ nm}$ in diameter). It presumably contains a high concentration of N atoms, and cannot simply be an amorphous GaAs region resulting from N implantation-induced damage, because the implantation temperature (380 °C) is much higher than the amorphous-to-crystalline transition temperature⁶ ($\approx 200 \text{ °C}$) of pure GaAs.

High-temperature anneals lead to transformation of these as-implanted precipitates into crystalline GaN [Fig. 1(c)]. The GaN precipitates are predominantly of the cubic phase, with a nearly cube-on-cube orientation relationship with the GaAs matrix, i.e., all lattice planes of the cubic GaN are nearly parallel to those of the GaAs of the same Miller indices [Fig. 1(d)]. The same result can also be obtained from selected-area diffraction (SAD) patterns e.g., Fig. 2, characterized by the alignment of the cubic GaN diffraction spots (indicated by arrows) with those from the GaAs (marked by black dots). For an 850 °C, 10 min anneal, additional weak

^{a)}Electronic mail: xwlin@ux5.lbl.gov

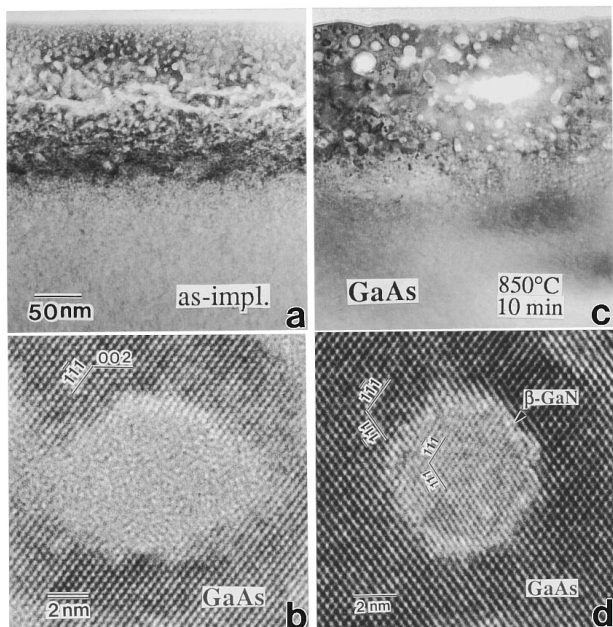


FIG. 1. Cross-sectional TEM micrographs of a GaAs sample implanted with 1.5×10^{17} N atoms cm^{-2} . (a) As-implanted; (b) high-resolution image of an amorphous precipitate from (a); (c) annealed at 850 °C for 10 min; (d) high-resolution image of a cubic GaN (β -phase) precipitate from (c). The images are viewed along GaAs [110].

diffraction rings were also observed, indicating the presence of some misoriented cubic GaN and some hexagonal GaN particles. The number of those particles appeared to decrease for extended anneals (850 °C for 2 h or 950 °C for 10 min). Not all the cubic GaN precipitates exhibited a perfect crystal structure is shown in Fig. 1(d); stacking faults were commonly observed.

Using the GaAs matrix as a reference, the lattice constant a_β of cubic GaN can be measured from both the high-resolution images [e.g., Fig. 1(d)] and SAD patterns (e.g., Fig. 2). A mean value of $a_\beta = 0.452$ nm, with a standard deviation of 0.2%, was determined for precipitates observed in different areas of one sample and in samples treated with various anneals. This value is nearly identical to that previ-

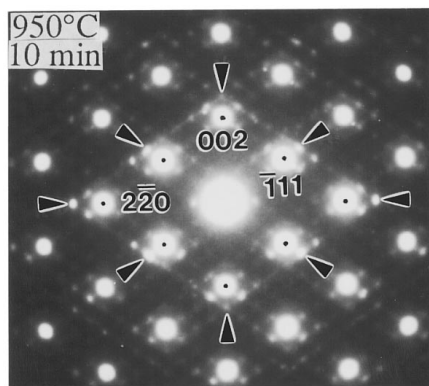


FIG. 2. SAD pattern of a N-implanted GaAs annealed at 950 °C for 10 min; implant fluence $= 1.5 \times 10^{17}$ cm^{-2} . Major diffraction spots from the GaAs and cubic GaN[110] zone axes are indicated by black dots and arrows, respectively. The weak satellite spots around the cubic GaN reflections are due to double diffraction.

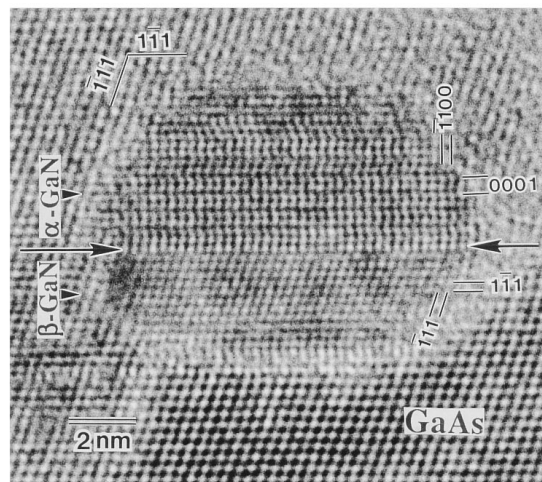


FIG. 3. High-resolution TEM micrograph showing coexistence of both hexagonal (α) and cubic (β) GaN phases in one precipitate, recorded from a 1.5×10^{17} N atoms cm^{-2} sample annealed at 950 °C for 40 min. The interface between the α and β GaN phases is indicated by arrows. The image is viewed along GaAs[110]|| α -GaN[11 $\bar{2}$ 0]|| β -GaN[110].

ously reported for cubic GaN epilayers grown on GaAs (001) substrates.³

Prolonged annealing at 950 °C causes a significant fraction of the cubic GaN precipitates to transform into the hexagonal phase (β - α phase transition), in addition to some precipitate coarsening. For a 40 min anneal, hexagonal GaN precipitates with a diameter greater than 25 nm were observed. A dramatic example of the β - α phase transition is shown in Fig. 3. Because the phase transition is incomplete, both the cubic and hexagonal GaN phases coexist in the one precipitate (≈ 10 nm in diameter), with the interphase boundary (indicated by arrows) parallel to their stacking planes, i.e., β -GaN(111)|| α -GaN(0001).

In order to produce a continuous GaN layer, the N implant fluence was doubled to 3×10^{17} cm^{-2} . The as-implanted sample [Figs. 4(a) and 4(b)] exhibits a layered structure, consisting of a continuous buried amorphous layer ≈ 80 nm thick between a surface layer ≈ 25 nm thick and a lower band (dark contrast) ≈ 55 nm wide, both of which contain amorphous precipitates.

Annealing results in an amorphous-to-crystalline transition with the formation of crystalline GaN. For an 850 °C, 10 min anneal, the as-implanted layered structure is essentially retained, but with a narrowing of the continuous layer from ≈ 80 to 50 nm thick and the upward migration of the lower precipitate region [Fig. 4(c)]. The most interesting finding is that the continuous layer consists of randomly oriented nanocrystals (≈ 5 nm in diameter) that are predominantly hexagonal GaN, while the precipitates in both the underlying region and the surface region are predominantly cubic GaN in epitaxy with the GaAs matrix. The latter is similar to the above low-fluence case (1.5×10^{17} cm^{-2}). Figure 4(d) shows a typical SAD pattern, recorded from the implanted area shown in Fig. 4(c). In addition to the diffraction rings from the hexagonal GaN layer, the diffraction spots from the epitaxial cubic GaN precipitates can also be seen (indicated by arrows). Similar results were also obtained for extended anneals (850 °C up to 2 h and 950 °C, 10 min).

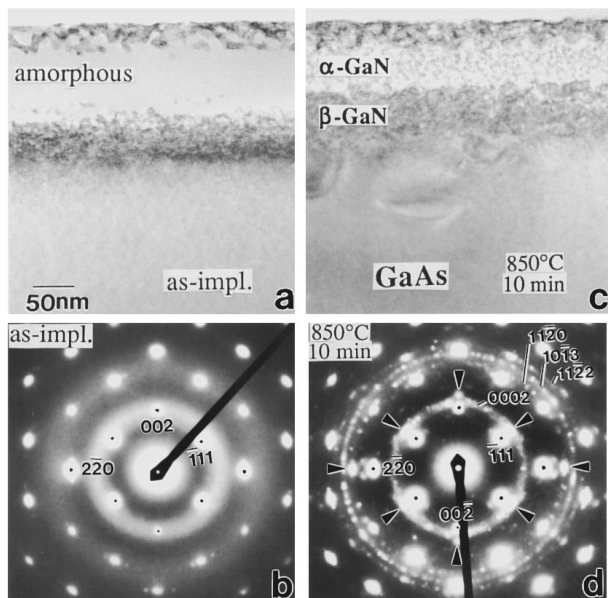


FIG. 4. Cross-sectional TEM micrographs of a GaAs sample implanted with 3×10^{17} N atoms cm^{-2} . (a) As-implanted and (b) the corresponding SAD pattern; (c) annealed at 850 °C for 10 min and (d) the corresponding SAD pattern. Diffraction spots from the GaAs[110] zone axis are marked by black dots. Note that the diffuse rings in (b) are due to the amorphous layer and precipitates in (a), while the diffraction rings (indexed with four-digit numbers) in (d) are due to reflections from the hexagonal GaN (α -phase) layer in (c). Note also that the reflections corresponding to the cubic GaN (β -phase) [110] zone axis (indicated by arrows) are due to the precipitates below and above the α -GaN layer.

The above observations suggest that interfacial energy plays a crucial role in determining the GaN phase. For precipitates formed in the GaAs matrix, the small particle size implies a relatively large interfacial area-to-volume ratio. By adopting the cubic GaN phase, rather than the hexagonal phase, the total free energy of the system is effectively minimized, because the cubic GaN and GaAs share the same crystal structure and presumably have a relatively low interfacial energy. On the other hand, the continuous layer crystallizes in the stable hexagonal GaN phase, because the interfacial area-to-volume ratio is substantially less and the GaN/GaAs interfacial energy is negligible. A similar phenomenon has also been observed for ion-beam synthesized FeSi_2 in Si.⁷

In order for GaN to be of practical use as a light emitting material, one must be able to produce thin films of high-quality single crystals; polycrystalline layers are *a priori* poor in both optical and electrical properties. Obviously, much work needs to be done to evaluate whether ion-beam synthesis can be used as a viable technique for GaN device applications. Nevertheless, the present study is of significance to the current GaN research in several aspects: First, it

presents a novel way of producing GaN. The use of conventional ion implantation techniques is of course costly to introduce a high concentration of N atoms in GaAs, but it can be replaced by relatively simple and cost-effective techniques such as plasma immersion ion implantation.⁸ Second, this study provides insight into the interaction of N plasma with GaAs. Previous studies⁵ indicated that N plasma treatment of a GaAs substrate at elevated temperatures results in the formation of a GaN surface layer, which is useful to promote vapor phase epitaxy of thick InN layers. Our TEM study provides direct evidence that GaN can be produced on GaAs via a N-As exchange mechanism. Finally, this letter shows that cubic GaN particles can be epitaxially formed in a GaAs matrix. Because of their small size (≈ 7.5 nm in diameter), these particles can be regarded as quantum dots and is of interest to fundamental research. Presumably, luminescence from GaN particles, stimulated by either a laser or an electron beam, is detectable, although the GaAs matrix may absorb a significant fraction of photons emitting from GaN, due to the fact that the former has a much smaller band gap than the latter. Work is in progress to systematically characterize the optical properties of ion-beam synthesized GaN.

In conclusion, we have successfully produced GaN in GaAs (001) by N ion implantation and subsequent thermal annealing. By varying the implant fluence, either hexagonal or cubic GaN phases can be produced, in the form of a continuous buried layer or epitaxial precipitates, respectively.

This work was supported by the Director, Office of Energy Research, Office of Basic Energy Sciences, Materials Science Division of the U.S. Department of Energy under Contract No. DE-AC03-76SF00098. The use of the facilities of the National Center for Electron Microscopy is acknowledged.

- ¹For a recent review on the subject, see H. Morkoç, S. Strite, G. B. Gao, M. E. Lin, B. Sverdlov, and M. Burns, *J. Appl. Phys.* **76**, 1363 (1994).
- ²J. H. Edgar, *J. Mater. Res.* **7**, 235 (1992); S. Strite and H. Morkoç, *J. Vac. Sci. Technol. B* **10**, 1237 (1992), and references therein.
- ³H. Okumura, S. Misawa, and S. Yoshida, *Appl. Phys. Lett.* **59**, 1058 (1991); S. Strite, J. Ruan, Z. Li, A. Salvador, H. Chen, D. J. Smith, W. J. Choyke, and H. Morkoç, *J. Vac. Sci. Technol. B* **9**, 1924 (1991).
- ⁴O. Kubaschewski and C. B. Alcock, *Metallurgical Thermochemistry*, 5th ed. (Pergamon, New York, 1979).
- ⁵L. A. DeLouise, *J. Vac. Sci. Technol. A* **11**, 609 (1993); Q. Guo, H. Ogawa, H. Yamano, and A. Yoshida, *Appl. Phys. Lett.* **66**, 715 (1995).
- ⁶S. J. Pearton, J. M. Poate, F. Sette, J. M. Gibson, D. C. Jacobson, and J. S. Williams, *Nucl. Instrum. Methods B* **19/20**, 369 (1987); A. Claverie, H. Fujioka, L. Laánab, Z. Liliental-Weber, and E. R. Weber, *Nucl. Instrum. Methods B* **96**, 327 (1995).
- ⁷X. W. Lin, M. Behar, J. Desimoni, H. Bernas, J. Washburn, and Z. Liliental-Weber, *Appl. Phys. Lett.* **63**, 105 (1993); X. W. Lin, J. Washburn, Z. Liliental-Weber, and H. Bernas, *J. Appl. Phys.* **75**, 4686 (1994).
- ⁸N. W. Cheung, *Nucl. Instrum. Methods B* **55**, 811 (1991).